

Gamma: Toward Generic Image Assessment with Mixture of Assessment Experts

Hantao Zhou
Tsinghua University
Shenzhen, China
hantaozh@outlook.com

Rui Yang
The University of Hong Kong
Hong Kong, China
rayyang0116@gmail.com

Longxiang Tang
Tsinghua University
Shenzhen, China
lloong.x@gmail.com

Guanyi Qin
National University of Singapore
Singapore, Singapore
guanyi.qin@u.nus.edu

Runze Hu*
Beijing Institute of Technology
Beijing, China
hrzlpk2015@gmail.com

Xiu Li
Tsinghua University
Shenzhen, China
li.xiu@sz.tsinghua.edu.cn

ABSTRACT

Image assessment aims to evaluate the quality and aesthetics of images and has been applied across various scenarios, such as natural and AIGC scenes. Existing methods mostly address these sub-tasks or scenes individually. While some works attempt to develop unified image assessment models, they have struggled to achieve satisfactory performance or cover a broad spectrum of assessment scenarios. In this paper, we present **Gamma**, a **Generic imAge assessMent** model using **Mixture of Assessment Experts**, which can effectively assess images from diverse scenes through mixed-dataset training. Achieving unified training in image assessment presents significant challenges due to annotation biases across different datasets. To address this issue, we first propose a Mixture of Assessment Experts (MoAE) module, which employs shared and adaptive experts to dynamically learn common and specific knowledge for different datasets, respectively. In addition, we introduce a Scene-based Differential Prompt (SDP) strategy, which uses scene-specific prompts to provide prior knowledge and guidance during the learning process, further boosting adaptation for various scenes. Our Gamma model is trained and evaluated on 12 datasets spanning 6 image assessment scenarios. Extensive experiments show that our unified Gamma outperforms other state-of-the-art mixed-training methods by significant margins while covering more scenes. Codes are available at <https://github.com/zht8506/Gamma>.

CCS CONCEPTS

• **Computing methodologies** → **Computer vision**.

KEYWORDS

Generic Image Assessment, Unified Training, Mixture of Experts

*Corresponding author.

Permission to make digital or hard copies of all or part of this work for personal or classroom use is granted without fee provided that copies are not made or distributed for profit or commercial advantage and that copies bear this notice and the full citation on the first page. Copyrights for components of this work owned by others than the author(s) must be honored. Abstracting with credit is permitted. To copy otherwise, or republish, to post on servers or to redistribute to lists, requires prior specific permission and/or a fee. Request permissions from permissions@acm.org.

MM '25, October 27-31, 2025, Dublin, Ireland

© 2025 Copyright held by the owner/author(s). Publication rights licensed to ACM.

ACM Reference Format:

Hantao Zhou, Rui Yang, Longxiang Tang, Guanyi Qin, Runze Hu, and Xiu Li. 2025. Gamma: Toward Generic Image Assessment with Mixture of Assessment Experts. In *Proceedings of the 33rd ACM International Conference on Multimedia (MM '25)*, October 27-31, 2025, Dublin, Ireland. ACM, New York, NY, USA, 13 pages.

1 INTRODUCTION

Image assessment is a long-standing research topic in the field of image processing, primarily comprising two tasks: Image Quality Assessment (IQA) and Image Aesthetic Assessment (IAA). These tasks require models to automatically evaluate the visual quality and aesthetic appeal of images, respectively. They have broad applications in various real-world scenarios, such as guiding image dehazing [80], selecting high-quality images in a data engine [46], serving as tools in an agentic system [68], or acting as reward models when aligning image generative models with human feedback [30].

Due to differences in image content and application scenarios, image assessment has spawned many sub-tasks, such as Natural-IQA for natural images, Face-IQA for facial images, AIGC-IQA for generated images, and IAA. Accordingly, numerous methods [18, 22, 50] have been proposed to address these specific tasks. However, these models often struggle to apply directly to other scenes or typically require task-specific fine-tuning on a given dataset. As illustrated in Figure 1, it is challenging for DEIQT [43] to transfer to other datasets without fine-tuning. This limitation prevents image assessment models from being widely applicable, e.g., IQA models are needed to assess facial, artistic, and natural images in the AIGC scene [30, 46, 68]. Hence, there is an urgent need for a model that can effectively handle a variety of scenarios.

To mitigate this issue, some approaches attempt to combine many datasets from various assessment tasks to train a general image assessment model. For instance, UNIQUE [76] and LIQE [77] utilize multiple authentic and synthetic natural IQA datasets for mixed training, but they focus only on natural image. Q-Align [59] uses a large language model with billions of parameters to unify IQA and IAA tasks, but it has a low inference speed and still solely focuses on natural images. PromptIQA [5] employs image-score pairs as prompts for quality predictions, but it is inflexible as it requires multiple images as references during inference. These methods fail

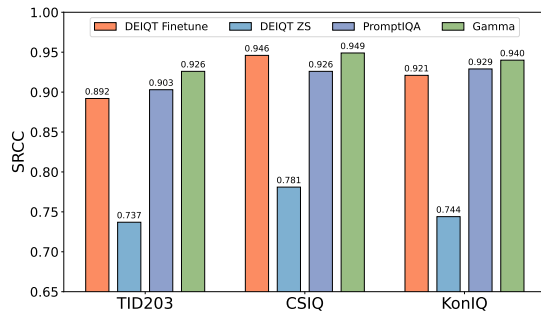


Figure 1: “DEIQT Finetune” is trained and tested on the same dataset. “DEIQT ZS” directly assesses images using the model trained on other datasets, which perform poorly. PromptQA and our Gamma are trained on mixed datasets. Our Gamma performs well on multiple datasets simultaneously and even surpass the task-specific method DETQT.

to cover a broad range of scenes and achieve competitive performance compared to models trained on specific datasets. Thus, it is imperative to develop an effective and generic image assessment model capable of evaluating images from various scenes.

To this end, we present **Gamma**, a **Generic imAge assessMent** model using **Mixture of Assessment** experts, to achieve unified image assessment across multiple scenes effectively. We found that the primary challenge in mixed-dataset training is *the mean opinion score (MOS) bias* between different datasets, e.g., images with similar MOS may exhibit different perceptual qualities across various datasets. As shown in Figure 2, samples from KonIQ [20], UWIQA [66], and SPAQ [10] show obvious differences in perceptual quality despite being labeled with similar MOS. To address this challenge, we introduce a novel **Mixture of Assessment Experts (MoAE)** module in our Gamma model. It consists of two types of experts: shared experts and adaptive experts. The shared experts are employed throughout to learn dataset-shared knowledge, while the adaptive experts are dynamically activated to varying degrees to learn dataset-specific knowledge. Additionally, an image-based router modulates the contributions of each adaptive expert. The MoAE allows the model to capture common features while flexibly adjusting representative features for different datasets. Compared with general Mixture of Experts (MoE) [47] and LoRA-based MoE [34], we equip the MoAE only in the rear blocks instead of all blocks, making it more efficient. Secondly, we propose a **Scene-based Differential Prompt (SDP)**, which uses different prompts for different datasets according to their scenes. This strategy provides scene-specific knowledge for representation learning of different datasets, guiding the mixed-dataset training process.

Our Gamma model is uniformly trained on a mixture of 12 datasets from 6 image assessment scenarios spanning IQA and IAA tasks. We then evaluate it on 12 datasets, demonstrating that it not only outperforms state-of-the-art (SOTA) mixed-training methods by notable margins, but also covers more scenarios. In some benchmarks, Gamma even surpasses some SOTA task-specific methods. Additionally, if we fine-tune our MoAE-equipped Gamma on specific datasets, it can achieve SOTA performance on 12 datasets.



Figure 2: Images with similar MOS labels from different datasets exhibit drastically different perceptual quality. It is not hard to observe that image (a) has clearly superior quality than the other three. Zoom in for a better view.

Moreover, the unified pre-trained Gamma can be utilized as a foundational model to significantly enhance other image assessment tasks, e.g., medical image quality assessment, and can achieve SOTA performance after task-specific training. In summary, our contributions are:

- We present **Gamma**, a powerful and generic image assessment model, capable of accurately assessing images from various scenarios through mixed training.
- We propose a novel Mixture of Assessment Experts (MoAE) module to extract representative features adaptively and a Scene-based Differential Prompt (SDP) strategy to provide guidance for representation learning, thereby achieving effective mixed-dataset training.
- Extensive experiments show that Gamma achieves SOTA performance on 12 datasets across 6 image assessment scenes in both mixed training and task-specific training settings.

2 RELATED WORK

2.1 Image Assessment

Image Assessment mainly includes two subtasks: Image Quality Assessment (IQA) and Image Aesthetic Assessment (IAA). In the deep learning era, these two tasks have achieved significant breakthroughs. For the IQA task, researchers develop various advanced techniques to improve performance, including feature and model structure design [71, 75], multi-level feature aggregation [2, 28, 63], adaptive convolution [52], transformer methods [22, 43], vision language models (VLMs) [57, 77] and large language models (LLM) [59, 72]. Moreover, besides the natural image assessment, there are various IQA methods for other scenes, such as face IQA [21, 40, 50], AIGC IQA [73], underwater IQA [16, 35, 65, 67]. For the IAA task, numerous methods have also been proposed to improve performance, including loss function [54], novel transformer architecture [56], multi-level features [19], theme information [18, 29] and multimodal pre-training [23].

2.2 Mixed Training for Image Assessment

As a fundamental image processing task, image assessment has been effectively applied to various scenarios. Recently, some works have attempted to develop unified methods that can be used in multiple IQA settings through mixed-dataset training. UNIQUE [76] sampled pairs of images from IQA datasets and computes the probability that the first image of each pair is of higher quality. StairIQA [53]

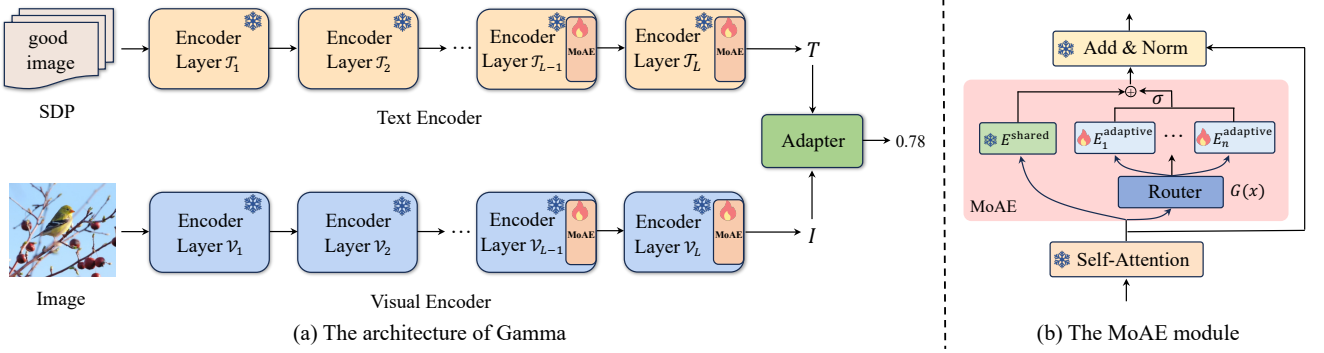


Figure 3: (a) The architecture of Gamma: It consists of a visual encoder \mathcal{V} and text encoder \mathcal{T} ; We add the Mixture of Assessment Experts (MoAE) to the last few layers of both encoders. We introduce a Scene-based Differential Prompt (SDP) to prompt images from different scenes (See Section 3.4 for details). (b) The MoAE module: It involves one shared expert (E^{shared}) and several adaptive experts (from E_1^{adaptive} to E_n^{adaptive}). We employ a router to adaptively activate the adaptive experts. We then use a learnable factor σ to merge the features of two type of experts.

designed separate IQA regression heads for each dataset. Prompt-IQA [5] utilized a short sequence of Image-Score Pairs as prompts for quality predictions. Q-Align [59] used large language model (LLM) to unify IQA and IAA tasks. However, most existing works fail to achieve competitive performance with task-specific methods and do not cover various scenes. Our Gamma outperforms other SOTA mixed-training methods by significant margins while covering more scenes.

2.3 Mixture of Experts

Mixture-of-Experts (MoE) divides specific parts of the parameters into several subsets, each of which is called an expert. It sets up a router that assigns experts to different inputs. Recently, the MoE structure has achieved remarkable success in large language models (LLM). For instance, DeepSeekMoE [8] proposes a novel MoE architecture that uses shared and routed experts to extract common and dynamic knowledge simultaneously. Beyond the natural language processing tasks, the idea of MoE has also been applied to vision models [4, 9, 45] and multimodal transformers [11, 58]. In Gamma, we utilize novel MoE module to effectively learn specific and general features of multi-dataset.

3 METHOD

3.1 Preliminary

As a foundational vision-language model (VLM), CLIP [44] has shown significant promise in supporting a wide array of vision tasks, including IQA and IAA tasks [41, 57, 78]. Specifically, CLIP is composed of a visual encoder \mathcal{V} and a text encoder \mathcal{T} , which generate aligned visual representations I and text representations T for each image-text pair. Utilizing these features, we can compute cosine similarity scores between image and text pairs across different domains or tasks to perform task-specific predictions, including image assessment tasks. Recently, to enhance CLIP’s capabilities in the field of image assessment, UniQA [82] fine-tuned CLIP on large-scale synthetic and authentic image-text datasets focused on image quality and aesthetics. This approach demonstrates excellent

performance on both IQA and IAA tasks after task-specific fine-tuning. However, the model lacks foundational applicability across various image assessment scenarios without fine-tuning. Building on the unified training pipeline proposed in UniQA, we propose two approaches to confront MOS bias present in different datasets and develop a foundational image assessment model. In the following, we will provide a detailed exposition of its components.

3.2 Overview of Gamma

As illustrated in Figure 3, our Gamma employs a visual encoder \mathcal{V} to extract visual features $I \in \mathbb{R}^d$, and a text encoder \mathcal{T} to extract text features $T \in \mathbb{R}^d$. After these encoders, a tunable adapter is used to obtain a score q representing image quality or aesthetics, following the methods in [77] and [82]. This process can be described as:

$$q = \sum_{k=1}^5 C_k \text{Softmax}(I'^T T_k / \tau), I' = \text{Adapter}(I), \quad (1)$$

where $\{T_k\}_{k=1}^5 \in \mathbb{R}^{5 \times d}$ represents text features of five assessment-dependent text prompts, *e.g.*, {bad image, poor image, fair image, good image, perfect image}. $\{C_k\}_{k=1}^5 \in \mathbb{R}^5$ is a learnable vector initialized to [0.2, 0.4, 0.6, 0.8, 1.0], and τ is a temperature parameter. In practice, the Adapter(\cdot) consists of two fully connected layers with a ReLU(\cdot) activation function in between. Based on this structure, to confront MOS bias in the mixed dataset and effectively perform unified pre-training, we propose a **Mixture of Assessment Experts (MoAE)** module to adaptively learn dataset-shared and dataset-specific knowledge from different datasets. We just integrate the MoAE into the last few layers of both encoders, as shown in Figure 3 (a). Notably, we only fine-tune the parameters of the MoAE modules, keeping the other parameters frozen, which is a significant advantage of our method. Additionally, we introduce a **Scene-based Differential Prompt (SDP)**. It uses different prompts for datasets from different scenes, thereby providing useful scene-based guidance for mixed-dataset training.

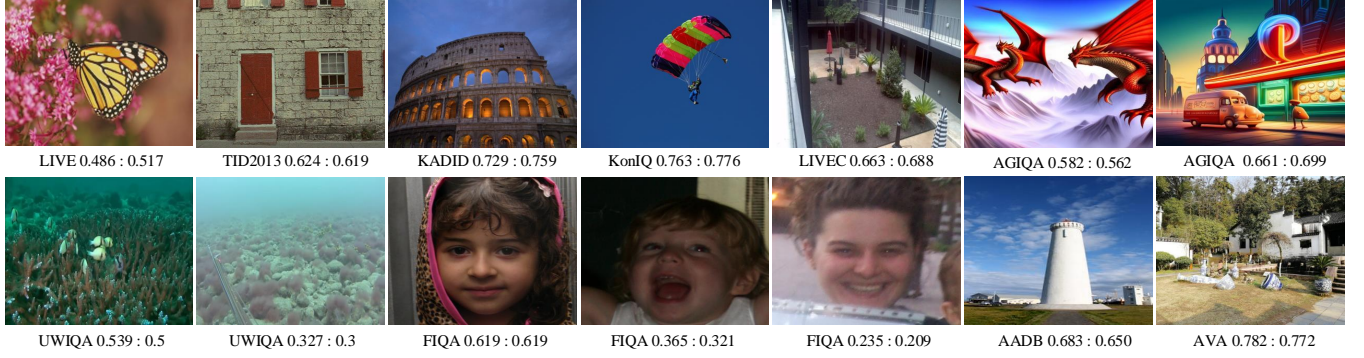


Figure 4: Visual examples from different datasets, which include natural images, underwater images, face images, AIGC images, and *etc.* The first value is the prediction score and the second value is the ground-truth MOS. Our Gamma accurately evaluates images from different scenes, demonstrating the generalization and effectiveness. All images are resized for better visibility.

3.3 Mixture of Assessment Experts

To develop a unified and generic image assessment model, we aim to combine multiple image assessment datasets for joint training. Unfortunately, the mean opinion score (MOS) introduces significant biases across different datasets, which hinders joint training. To address this challenge, we propose the MoAE module, where several experts are employed to learn the diverse biases of different datasets. As shown in Figure 3 (b), the MoAE includes a shared assessment expert (E^{shared}) to learn common knowledge of image assessment and several adaptive assessment experts (from E_1^{adaptive} to E_n^{adaptive}) to dynamically learn dataset-specific knowledge.

The Shared Assessment Expert. The shared assessment expert E^{shared} inherits the image assessment capabilities of the original multimodal model (e.g., CLIP [44] or UniQA [82]) by reusing its weights. This expert remains frozen during training to ensure that the learned world knowledge is retained. Thus, the model can capture common representations across various contexts and maintain its original multi-modal capabilities. Given an input hidden state $x \in \mathbb{R}^d$, the output of the shared assessment expert is:

$$y^{\text{shared}} = E^{\text{shared}}(x), \quad (2)$$

where $E^{\text{shared}}(\cdot)$ is implemented as the original feed-forward network (FFN) of the CLIP model.

The Adaptive Assessment Expert. The adaptive assessment expert module contains two components: (1) n experts $\{E_i^{\text{adaptive}}\}_{i=1}^n$ to capture diverse facets of multi-dataset information; and (2) a router $G(\cdot)$ to tailor the contribution of different experts based on the input feature. Given an input feature $x \in \mathbb{R}^d$, the output y^{adaptive} can be computed as:

$$y^{\text{adaptive}} = \sum_{i=1}^n G(x)_i E_i^{\text{adaptive}}(x), \quad (3)$$

$$G(x) = \text{Softmax}(Wx).$$

Here, the router $G(\cdot)$ is a linear transformation for the input feature x ; $W \in \mathbb{R}^{n \times d}$ is the transformation matrix. We utilize a Softmax operator to normalize the contribution weights. Notably, we initialize these experts with the weights of pre-trained multimodal model to equip them with preliminary image assessment capabilities.

MoAE Module. Based on the above experts, the MoAE module merges the features of the two types of experts with a learnable factor σ , as shown on the right side of Figure 3. Thus, the output of the MoAE module can be expressed as:

$$y^{\text{MoAE}} = y^{\text{shared}} + \sigma \cdot y^{\text{adaptive}}. \quad (4)$$

The σ factor is zero-initialized so that the visual and text encoders can generate aligned features at the beginning of training. We freeze the shared experts and set the adaptive experts to be tunable only. This approach preserves the learned knowledge of the original model and improves training efficiency.

Inspired by [64], which points out that higher layers are easier to tune for downstream tasks and freezing lower layers preserves more generalizable knowledge, we incorporate the MoAE into the last K layers of both visual and text encoders, as shown in Figure 3. This strategy makes our method both effective and efficient. The visual feature extraction process can be formulated as:

$$I_i = \mathcal{V}_i(I_{i-1}), \quad i = 1, 2, \dots, L - K$$

$$I_j = \mathcal{V}_j^{\text{MoAE}}(I_{j-1}), \quad j = L - K + 1, \dots, L \quad (5)$$

where L denotes the number of layers of the visual encoder; I_i represents the visual features of the i -th encoder layer; and $\mathcal{V}^{\text{MoAE}}$ represents the MoAE-equipped visual encoder layer. The text branch operates similarly to the visual branch.

3.4 Scene-based differential prompt

To facilitate scene-guided learning, we introduce a **Scene-based Differential Prompt (SDP)** to help the model acquire scene-specific knowledge from different datasets. We utilize 12 datasets spanning 6 image assessment scenarios, including synthetic distortion Natural IQA, authentic distortion Natural IQA, face IQA, AIGC IQA, underwater IQA, and IAA, for mixed training. We categorize these datasets into five groups based on their scenes: natural quality, AI-generated quality, underwater quality, face quality, and natural aesthetics. Specifically, for the face quality assessment dataset, we use prompts such as *face bad-quality*, *face poor-quality*, *face fair-quality*, *face good-quality*, *face perfect-quality* appended to the word *image*. Then, the text prompt is sent to the text encoder of the Gamma to obtain text features. Text features will be combined

Table 1: Comparison with SOTA task-specific and mixed-training models on 12 datasets for 6 image assessment tasks. “Gamma” and “Gamma-T” denote the mixed-training and task-specific models, respectively. Gamma[†] uses the Scene-based Differential Prompt (SDP) for training and testing. * indicates that we retrain the model with the same data split as ours.

Task	Synthetic Distortion Natural IQA (SDN-IQA)						Authentic Distortion Natural IQA (ADN-IQA)								
Training	Dataset	LIVE		CSIQ		TID2013		KADID		LIVEC		KonIQ		SPAQ	
Type	Method	SRCC	PLCC	SRCC	PLCC	SRCC	PLCC	SRCC	PLCC	SRCC	PLCC	SRCC	PLCC	SRCC	PLCC
Task Specific	HyperIQA	0.962	0.966	0.923	0.942	0.840	0.858	0.852	0.845	0.859	0.882	0.906	0.917	0.911	0.915
	MUSIQ	0.940	0.911	0.871	0.893	0.773	0.815	0.875	0.872	0.702	0.746	0.916	0.928	0.918	0.921
	TOPIQ	0.943	0.942	0.908	0.925	0.813	0.845	0.877	0.875	0.833	0.868	0.915	0.925	0.914	0.917
	DEIQT	0.980	0.982	0.946	0.963	0.892	0.908	0.889	0.887	0.875	0.894	0.921	0.934	0.919	0.923
	LoDA	0.975	0.979	-	-	0.869	0.901	0.931	0.936	0.876	0.899	0.932	0.944	0.925	0.928
	UniQA	0.981	0.983	0.963	0.973	0.916	0.931	0.940	0.943	0.890	0.905	0.933	0.941	0.924	0.928
	Gamma-T	0.982	0.971	0.973	0.978	0.944	0.950	0.960	0.961	0.899	0.921	0.945	0.952	0.928	0.931
Mixed Training	UNIQUE	0.969	0.968	0.902	0.927	-	-	0.878	0.876	0.854	0.890	0.896	0.901	-	-
	LIQE*	0.972	0.953	0.946	0.943	-	-	0.932	0.933	0.902	0.908	0.920	0.905	-	-
	StairIQA	0.937	0.934	0.768	0.843	0.675	0.773	0.785	0.805	0.780	0.855	0.865	0.896	0.903	0.907
	PromptIQA	0.936	0.934	0.926	0.939	0.903	0.922	0.928	0.931	0.913	0.928	0.929	0.943	0.923	0.926
	Gamma	0.957	0.952	0.949	0.966	0.926	0.934	0.960	0.962	0.851	0.871	0.940	0.949	0.923	0.928
	Gamma [†]	0.953	0.953	0.960	0.968	0.935	0.941	0.962	0.964	0.891	0.914	0.939	0.950	0.929	0.932

Task	Face IQA (F-IQA)			AIGC IQA (AG-IQA)			Underwater IQA (U-IQA)			Image Aesthetic Assessment (IAA)					
Training	Dataset	GFQA20k		Dataset	AGQA3k		Dataset	UWIQA		Dataset	AVA		Dataset	AADB	
Type	Method	SRCC	PLCC	Method	SRCC	PLCC	Method	SRCC	PLCC	Method	SRCC	PLCC	Method	SRCC	PLCC
Task Specific	IFQA	0.960	0.960	DBCNN	0.821	0.876	FDUM	0.694	0.689	MaxViT	0.708	0.745	MUSIQ	0.706	0.712
	StyleGAN	0.967	0.968	HyperNet	0.836	0.890	UCIQE	0.627	0.626	TANet	0.758	0.765	TANet	0.738	0.737
	TOPIQ	0.966	0.967	CLIPQA	0.843	0.805	URanker	0.674	0.663	VILA	0.774	0.774	TAVAR	0.761	0.763
	CR-FQA	0.959	0.960	MUSIQ	0.826	0.866	UIQI	0.742	0.741	ELTA	0.764	0.777	ELTA	0.760	0.772
	GPFIQA	0.964	0.965	PSCR	0.850	0.906	HPUIQA	0.796	0.790	UniQA	0.776	0.776	UniQA	0.786	0.787
	Gamma-T	0.968	0.968	Ours-T	0.894	0.921	Ours-T	0.870	0.880	Ours-T	0.785	0.784	Ours-T	0.793	0.798
Mixed Training	UNIQUE	-	-	UNIQUE	-	-	UNIQUE	-	-	UNIQUE	-	-	UNIQUE	-	-
	LIQE	-	-	LIQE	-	-	LIQE	-	-	LIQE	-	-	LIQE	-	-
	StairIQA	0.937	0.935	StairIQA	0.755	0.833	StairIQA	0.722	0.727	StairIQA	-	-	StairIQA	-	-
	PromptIQA	0.970	0.971	PromptIQA	0.851	0.901	PromptIQA	0.877	0.884	PromptIQA	-	-	PromptIQA	-	-
	Gamma	0.970	0.970	Gamma	0.870	0.910	Gamma	0.863	0.878	Gamma	0.740	0.737	Gamma	0.742	0.743
	Gamma [†]	0.970	0.970	Gamma [†]	0.887	0.923	Gamma [†]	0.873	0.884	Gamma [†]	0.750	0.749	Gamma [†]	0.756	0.755

with image features for quality prediction (Section 3.2). For more details on these prompts, please refer to Supplementary Materials.

This strategy effectively differentiates the feature space of images from various scenes and enhances scene-specific knowledge, thereby mitigating the MOS bias across different datasets. Experimental results show that this method significantly improves the model’s performance (Table 1).

4 EXPERIMENTS

4.1 Datasets

We utilize 12 datasets for unified training and testing, encompassing both IQA and IAA tasks. For the IQA task, five different assessment scenarios are included: synthetic distortion natural IQA (SDN-IQA), authentic distortion natural IQA (ADN-IQA), face IQA (F-IQA), AIGC IQA (AG-IQA), and underwater IQA (U-IQA). For the IAA task, we use two classical benchmarks, AVA and AADB. In addition, we use two rare datasets to verify the generalization ability of the model, *i.e.*, exBeDDE and ECIQAD. The exBeDDE is a dehazed image quality assessment (D-IQA) dataset, and the ECIQAD is an enhanced colonoscopy image quality assessment (EC-IQA) dataset. Details about these datasets is provided in supplementary materials.

4.2 Implementation Details

Following the settings in [22, 52], we randomly divide each dataset into 80% for training and 20% for testing. The training dataset is a mixture of the training sets of each dataset and we test Gamma on each test data separately. This process is repeated 10 times, and the median of the 10 scores is reported as the final score. We use the pre-trained weight of UniQA [82], which uses CLIP-B/16 as multimodal encoder. We freeze the CLIP visual and text encoders, training only the MoAE module and adapter. For the unified training, we train the model for 10 epochs with a batch size of 8. The initial learning rate is set to $2e-5$. We normalize the MOS/DMOS scale to $[0, 1]$ and utilize Adam optimizer [24] and MSE loss to optimize the model. For the task-specific training, we use different training settings according to the task and size of datasets. More training details are provided in the supplementary materials.

4.3 Main Results

Our MoAE-equipped model can be used for task-specific training and mixed training, both of which can achieve state-of-the-art (SOTA) performance, as shown in Table 1. We conduct a comprehensive performance comparison of the Gamma with 30 SOTA IQA methods on the 6 IQA tasks. We compare natural scene IQA methods, including HyperIQA [52], MUSIQ [22], TOPIQ [2], DEIQT [43],

Table 2: The effect of Mixture of Assessment Experts (MoAE) and Scene-based Differential Prompt (SDP).

Dataset		LIVEC		KonIQ		LIVE		CSIQ		AGIQA3k		UWIQA		AVA	
MoAE	SDP	SRCC	PLCC	SRCC	PLCC	SRCC	PLCC	SRCC	PLCC	SRCC	PLCC	SRCC	PLCC	SRCC	PLCC
×	×	0.765	0.792	0.858	0.885	0.927	0.918	0.852	0.898	0.800	0.866	0.750	0.768	0.681	0.672
×	✓	0.843	0.856	0.874	0.896	0.929	0.917	0.866	0.901	0.841	0.887	0.770	0.780	0.721	0.715
✓	×	0.851	0.871	0.940	0.949	0.957	0.952	0.949	0.966	0.870	0.910	0.863	0.878	0.740	0.737
✓	✓	0.891	0.914	0.939	0.950	0.960	0.968	0.953	0.953	0.887	0.923	0.873	0.884	0.750	0.749

Table 3: The impact of different number of experts in adaptive experts. We use naive prompt strategy for ablation.

Dataset	LIVEC		CSIQ		TID2013		AGIQA3k		UWIQA		Average	
Experts Number	SRCC	PLCC	SRCC	PLCC	SRCC	PLCC	SRCC	PLCC	SRCC	PLCC	SRCC	PLCC
Zero Expert	0.765	0.792	0.852	0.898	0.792	0.826	0.800	0.866	0.750	0.768	0.792	0.83
One Expert	0.842	0.866	0.945	0.963	0.918	0.931	0.866	0.908	0.859	0.873	0.886	0.908
Three Experts	0.851	0.871	0.949	0.966	0.926	0.934	0.870	0.910	0.863	0.878	0.892	0.912
Five Experts	0.854	0.889	0.951	0.965	0.926	0.934	0.872	0.911	0.860	0.876	0.893	0.915

Table 4: The impact of different model configuration in the proposed MoAE module.

Dataset	LIVEC		CSIQ		AGIQA3k		UWIQA		AVA	
Model Configuration	SRCC	PLCC	SRCC	PLCC	SRCC	PLCC	SRCC	PLCC	SRCC	PLCC
Unfreeze shared expert	0.849	0.869	0.946	0.957	0.864	0.904	0.858	0.871	0.720	0.719
w/o Merging factor σ	0.847	0.866	0.932	0.947	0.851	0.903	0.845	0.869	0.698	0.697
Our MoAE module	0.851	0.871	0.949	0.966	0.870	0.910	0.863	0.878	0.740	0.737

LoDA [63], UniQA [82], UNIQUE [76], LIQE [77], StairQA [53] and PromptIQA [5]; face IQA methods, including IFQA [21], StyleGAN-IQA from [50], CR-FIQA [1], GPFIQA [50]; AIGC IQA methods, including DBCNN [75], CLPIQA [57] and PSCR [73]; underwater IQA methods, including FDUM [66], UIQI [35], URanker [16], UCIQE [65] and HPUIQA [35], and IAA methods, including VILA [23], TANet [18], MaxViT [56], TAVAR [29] and ELTA [32].

Task-specific Training. We apply our method to 12 image assessment datasets. We use the fixed naive prompt (described in Section 3.2) for training and testing. We observe that our method outperforms all others methods by a significant margin. On some benchmark, our method achieve dramatic improvements, such as SRCC of 0.944 (v.s. 0.916) on TID2013 and 0.945 (v.s. 0.933) on KonIQ. Since images in these 12 datasets encompass a wide variety of contents and distortion types, it is particularly challenging to consistently achieve the leading performance on all of them.

Mixed Training. We conduct mixed training on 12 image assessment datasets. The trained model can be used to assess the images from these datasets directly. The experimental results are reported in Table 1. When compared with other mixed training models, our method exhibits competitive results on each dataset. More importantly, our method can also be used to IAA tasks and demonstrates excellent performance. It is worth noting that our mixed training model even achieves results comparable to task-specific models on datasets such as KADID, KonIQ, SPAQ, and GFIQA. These results demonstrate that our approach can be effectively applied to different image assessment scenarios.

Qualitative Results. We visualize the image assessment results from different datasets, covering various scenarios, as shown in Figure 4. We can notice that our Gamma can accurately assess images from various tasks. These results shows the high generalization capability of our Gamma.

4.4 Ablation Studies

We conduct detailed ablation studies to validate the effectiveness of our modules. Note that we use naive prompt strategy (described in Section 3.2) to perform all ablations unless otherwise specified. We uniformly use 12 datasets for ablation experiments. Considering the page limit, we only show the datasets with relatively large differences in results. More ablations about prompt sensitivity and model efficiency please refer to Supplementary Materials.

Effectiveness of the prompt strategy. We propose the Scene-based Differential Prompt (SDP) to prompt different datasets. We evaluate the effectiveness of this strategy in Table 1. We can notice that the SDP strategy can improve the model performance on multiple datasets, especially on CSIQ (+1.1% SRCC), LIVEC (+4% SRCC) and AGIQA-3k (+1.7 % SRCC). These results demonstrate that the SDP can effectively guide model learn differential features for different datasets, thus enhancing model performance. Furthermore, we ablate the SDP strategy and MOAE module respectively to explore their relationship and impact on model performance. As shown in Table 2, both methods can improve the performance of the model, such as +7.8% SRCC of SDP and +8.6% SRCC of MoAE on LIVEC. This shows the effectiveness of this adaptive expert feature learning and text guidance for multi-dataset learning. When the

Table 5: The impact of adding MoAE to different numbers of layers for training. Time means training time.

Dataset	Parms	Time	LIVEC		KonIQ		LIVE		CSIQ		AGIQA3k		UWUQA		AVA	
			SRCC	PLCC	SRCC	PLCC	SRCC	PLCC	SRCC	PLCC	SRCC	PLCC	SRCC	PLCC	SRCC	PLCC
MoE Layer	Million	Hours														
w/o MoAE	149.9	3.5	0.765	0.792	0.858	0.885	0.927	0.918	0.852	0.898	0.800	0.866	0.750	0.768	0.681	0.672
Last 4 layers	231.8	7.5	0.830	0.859	0.933	0.944	0.954	0.952	0.937	0.960	0.866	0.909	0.853	0.867	0.735	0.732
Last 6 layers	272.7	10.2	0.851	0.871	0.940	0.949	0.957	0.952	0.949	0.966	0.870	0.910	0.863	0.878	0.740	0.737
Last 8 layers	313.6	13.4	0.852	0.883	0.941	0.947	0.956	0.951	0.953	0.967	0.872	0.913	0.866	0.875	0.746	0.743
All 12 layers	395.5	17.2	0.860	0.883	0.939	0.950	0.954	0.950	0.954	0.968	0.881	0.908	0.863	0.868	0.728	0.725

Table 6: Results when only one adaptive expert is activated. The weights factors of other experts are set to 0. It can be observed that different experts focus on different datasets.

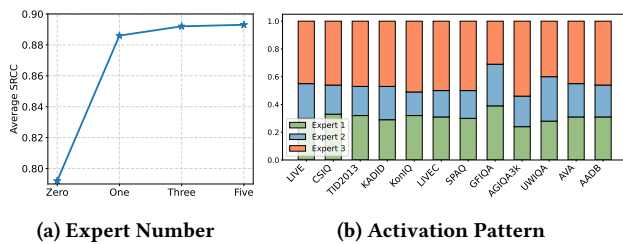
Dataset	LIVEC		KonIQ		LIVE		CSIQ		AGIQA3k		UWUQA		GFIQA		AVA	
	SRCC	PLCC														
Expert index																
1-th expert	0.847	0.860	0.927	0.938	0.933	0.933	0.894	0.906	0.815	0.870	0.770	0.779	0.959	0.957	0.666	0.673
2-th expert	0.715	0.672	0.681	0.717	0.900	0.861	0.815	0.846	0.832	0.885	0.755	0.756	0.826	0.797	0.663	0.652
3-th expert	0.768	0.741	0.794	0.818	0.918	0.917	0.833	0.877	0.808	0.910	0.691	0.709	0.903	0.897	0.715	0.716
Gamma	0.851	0.871	0.940	0.949	0.957	0.952	0.949	0.966	0.870	0.910	0.863	0.878	0.970	0.970	0.740	0.737

Table 7: Comparison with LIQE [77] and UNIQUE [76] when using the same training data.

Dataset	LIVE		CSIQ		KADID		BID		LIVEC		KonIQ		Average	
	SRCC	PLCC	SRCC	PLCC										
Method														
UNIQUE	0.961	0.952	0.902	0.921	0.884	0.885	0.852	0.875	0.854	0.884	0.895	0.900	0.891	0.903
LIQE	0.970	0.951	0.936	0.939	0.930	0.931	0.875	0.900	0.904	0.910	0.919	0.908	0.922	0.923
Gamma [†]	0.960	0.947	0.936	0.957	0.955	0.956	0.901	0.925	0.890	0.915	0.933	0.946	0.929	0.941

Table 8: Comparison with Q-Align [59] when using the same training data.

Dataset	KonIQ		SPAQ		KADID		Average	
	SRCC	PLCC	SRCC	PLCC	SRCC	PLCC	SRCC	PLCC
Method								
Q-Align	0.938	0.945	0.931	0.933	0.934	0.935	0.934	0.938
Gamma [†]	0.940	0.950	0.928	0.932	0.962	0.964	0.943	0.949

**Figure 5: (a) Average performance when using different numbers of experts. Adding adaptive experts significantly improves model performance. (b) Average activations of three experts in the last layer of the visual encoder. Image evaluations of different scenes have different activation patterns.**

two methods are used simultaneously, the model can achieve the best results. Therefore, the two methods are mutually beneficial. **The number of experts.** We explore the impact of different numbers of experts in the adaptive assessment experts. As shown in

Table 3 and Figure 5a, the model achieves higher performance with more experts. This suggests that adding experts can better cope with the dataset bias problem when using a mixed training strategy. Using five experts cannot significantly improve the performance as the performance approaches saturation. We use three experts to constitute the adaptive assessment experts in MoAE to achieve the optimal trade-off between accuracy and efficiency.

Effect of freezing the shared expert. We freeze the shared expert in the MoAE to retrain the multimodal capability of original model. This strategy also helps model capture the generalizable and common representation across varying contexts. Table 4 validates this method and shows that it is effective across various datasets.

Merging features with factor σ . Table 4 also demonstrates the effect of merging features of shared and adaptive experts with factor σ . We notice that this strategy improves the model performance on different datasets, especially on AVA and AGIQA3k. These results show that it is beneficial to utilize aligned features at the beginning of training and partially using features from adaptive experts. We plot the value change of σ during training in Figure 6. The absolute value of σ increases gradually and eventually stabilize. This means that the adaptive expert is constantly fitting the bias between different datasets. The value is negative, suggesting that the adaptive experts remove the preference scores from the shared expert, similar to a denoising process.

Adding adapter to last few layers. We add the proposed MoAE module into the last few layers of the visual and text encoders. We compare the performance of adding MoAE to different numbers

Table 9: Generalization capability validation on the exBeDDE and ECIQAD datasets. The “Pretrained weight” denotes the model weight of mixed training. Loading pretrained weight for initialization improves model performance.

(a) Results on the exBeDDE dataset.		
Method	SRCC	PLCC
BRISQUE [38]	0.890	0.906
PSQA-I [33]	0.907	0.924
HyperIQA [52]	0.917	0.926
FADE [6]	0.714	0.729
DHQI [37]	0.919	0.939
VDA-DQA [15]	0.923	0.942
Ours	0.916	0.938
Ours + Pretrained weight	0.937	0.951
(b) Results on the ECIQAD dataset.		
Method	SRCC	PLCC
BRISQUE [38]	0.436	0.459
BIQME [14]	0.770	0.768
BPRI [36]	0.152	0.181
FRIQUEE [13]	0.663	0.656
CIQA [3]	0.738	0.735
ECIQ [22]	0.839	0.842
Ours	0.912	0.922
Ours + Pretrained weight	0.917	0.927

of layers in Table 5. After using MoAE, the performance of the model is significantly improved. We also observe that adding more than six layers of adapters does not improve model performance significantly, but further increases the model parameter and training overhead. Therefore, we integrate MoAE module in the last six layers of both visual and text encoder.

Activation patterns of different datasets. We visualize the average activation degree of three experts in the last layer of Gamma’s visual encoder for different datasets, as shown in Figure 5b. We observe that the activation patterns are different for different scenarios. Specifically, the natural IQA datasets, *e.g.*, LIVE, CSIQ, KADID, show different activation patterns from the face IQA dataset GFIQA and the underwater IQA dataset UWIQA. The synthetic and authentic distortion datasets in natural IQA also have different activation patterns. These indicate that our MoAE module can assign experts with different activation levels to images of different scenarios, thereby capturing the discriminative features effectively.

Analysis of the adaptive experts. We add an experiment in which we only use one adaptive expert and set the router weights of the other experts to 0, to explore the preferences of different experts for different datasets. As shown in Table 6, the first expert performs well on most datasets, indicating it learns a general image assessment ability. The second and third experts focus on AIGC IQA and IAA tasks, respectively, and the third expert also shows excellent evaluation capabilities for natural images. These results indicate that different experts have learned domain-specific features of different datasets. They collaborate to achieve the powerful image assessment model Gamma.

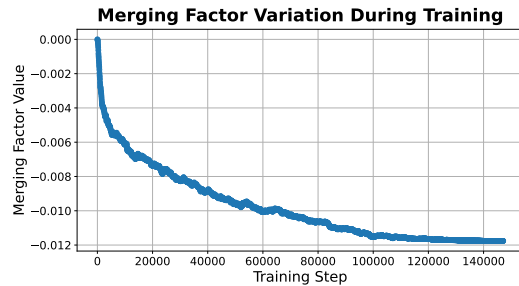


Figure 6: The change of merging factor σ during training. The σ is from the MoAE of the last visual encoder layer.

4.5 Comparison with Mixed Training Methods

In this subsection, we conduct a more detailed comparison with other mixed training methods. We first compare with LIQE and UNIQUE using the same training data and data splitting ratios. As shown in Table 7, our method achieves better performance on most datasets than LIQE and UNIQUE, especially on the KADID (+2.5% SRCC) and BID (+2.6% SRCC) datasets compared with LIQE. On other datasets, *i.e.*, LIVE and LIVEC, our model also achieves competitive results. Overall, our model has superior performance on these five datasets. Compared with Q-Align, as shown in Table 8, our method achieves better results on KonIQ and KADID, and is also highly competitive on SPAQ.

4.6 Generalization Capability Validation

We further validate the generalization capability of our method on two datasets, exBeDDE and ECIQAD. The exBeDDE is a dehazed IQA dataset and the ECIQAD is an enhanced colonoscopy IQA dataset, which belong to completely different domains compared to the used datasets in mixed training. We use naive prompt strategy for training and testing. The experimental results are reported in Table 9. We notice that our method can achieve competitive performance on these two datasets, showing the effectiveness and generalization capability of our method. More importantly, when we load the pretrained weight of Gamma for initialization, the performance of both datasets is improved and our method achieves the SOTA results. This indicates that our pretrained Gamma can be an effective foundation model to aid other assessment fields.

5 CONCLUSION

This paper introduces Gamma, a generic image assessment model that can be applied to various image scenarios. To achieve this, we utilize the mixed training of different datasets to obtain the assessment abilities of different scenarios. We propose a Mixture of Assessment Expert (MoAE) module and a Scene-based Differential Prompt (SDP) strategy to effectively cope with the MOS bias in different datasets. MoAE utilizes shared experts and adaptive experts to extract common and representative features adaptively. SDP strategy employs different prompts for different datasets to provide guidance for feature learning. Extensive experiments demonstrate that our method can achieve SOTA performance on various datasets simultaneously, showing the strong generalization and general image assessment capabilities.

REFERENCES

- [1] Fadi Boutros, Meiling Fang, Marcel Klemm, Biying Fu, and Naser Damer. 2023. CR-FQA: face image quality assessment by learning sample relative classifiability. In *Proceedings of the IEEE/CVF conference on computer vision and pattern recognition*. 5836–5845.
- [2] Chaofeng Chen, Jiadi Mo, Jingwen Hou, Haoning Wu, Liang Liao, Wenxiu Sun, Qiong Yan, and Weisi Lin. 2024. Topiq: A top-down approach from semantics to distortions for image quality assessment. *IEEE Transactions on Image Processing* (2024).
- [3] Hangwei Chen, Xiongli Chai, Feng Shao, Xuejin Wang, Qiuping Jiang, Xiangchao Meng, and Yo-Sung Ho. 2021. Perceptual quality assessment of cartoon images. *IEEE Transactions on Multimedia* 25 (2021), 140–153.
- [4] Tianlong Chen, Xuxi Chen, Xianzhi Du, Abdullah Rashwan, Fan Yang, Huizhong Chen, Zhangyang Wang, and Yeqing Li. 2023. Adamv-moe: Adaptive multi-task vision mixture-of-experts. In *Proceedings of the IEEE/CVF International Conference on Computer Vision*. 17346–17357.
- [5] Zewen Chen, Haina Qin, Juan Wang, Chunfeng Yuan, Bing Li, Weiming Hu, and Liang Wang. 2024. PromptQA: Boosting the Performance and Generalization for No-Reference Image Quality Assessment via Prompts. *arXiv preprint arXiv:2403.04993* (2024).
- [6] Lark Kwon Choi, Jaehye You, and Alan Conrad Bovik. 2015. Referenceless prediction of perceptual fog density and perceptual image defogging. *IEEE Transactions on Image Processing* 24, 11 (2015), 3888–3901.
- [7] Xiaohui Chu, Hantao Zhou, Yan Zhang, Yachao Zhang, Runze Hu, Haoran Duan, Yawen Huang, Yefeng Zheng, and Rongrong Ji. 2025. Attention-driven acoustic properties learning for underwater target ranging. *Pattern Recognition* 164 (2025), 111560.
- [8] Damai Dai, Chengqi Deng, Chenggang Zhao, RX Xu, Huazuo Gao, Deli Chen, Jiashi Li, Wangding Zeng, Xingkai Yu, Y Wu, et al. 2024. Deepseekmoe: Towards ultimate expert specialization in mixture-of-experts language models. *arXiv preprint arXiv:2401.06066* (2024).
- [9] Yongxing Dai, Xiaotong Li, Jun Liu, Zekun Tong, and Ling-Yu Duan. 2021. Generalizable person re-identification with relevance-aware mixture of experts. In *Proceedings of the IEEE/CVF conference on computer vision and pattern recognition*. 16145–16154.
- [10] Yuming Fang, Hanwei Zhu, Yan Zeng, Kede Ma, and Zhou Wang. 2020. Perceptual quality assessment of smartphone photography. In *CVPR*. 3677–3686.
- [11] Zhida Feng, Zhenyu Zhang, Xintong Yu, Yewei Fang, Lanxin Li, Xuyi Chen, Yuxiang Lu, Jiaxiang Liu, Weichong Yin, Shikun Feng, et al. 2023. Ernie-vilg 2.0: Improving text-to-image diffusion model with knowledge-enhanced mixture-of-denoising-experts. In *Proceedings of the IEEE/CVF Conference on Computer Vision and Pattern Recognition*. 10135–10145.
- [12] Deepti Ghadiyaram and Alan C Bovik. 2015. Massive online crowdsourced study of subjective and objective picture quality. *IEEE TIP* 25, 1 (2015), 372–387.
- [13] Deepti Ghadiyaram and Alan C Bovik. 2017. Perceptual quality prediction on authentically distorted images using a bag of features approach. *Journal of vision* 17, 1 (2017), 32–32.
- [14] Ke Gu, Dacheng Tao, Jun-Fei Qiao, and Weisi Lin. 2017. Learning a no-reference quality assessment model of enhanced images with big data. *IEEE transactions on neural networks and learning systems* 29, 4 (2017), 1301–1313.
- [15] Tuxin Guan, Chaofeng Li, Ke Gu, Hantao Liu, Yuhui Zheng, and Xiao-jun Wu. 2022. Visibility and distortion measurement for no-reference dehazed image quality assessment via complex contourlet transform. *IEEE Transactions on Multimedia* 25 (2022), 3934–3949.
- [16] Chunle Guo, Ruiqi Wu, Xin Jin, Linghao Han, Weidong Zhang, Zhi Chai, and Chongyi Li. 2023. Underwater ranker: Learn which is better and how to be better. In *Proceedings of the AAAI conference on artificial intelligence*, Vol. 37. 702–709.
- [17] Shuai He, Anlong Ming, Yaqi Li, Jinyuan Sun, ShunTian Zheng, and Huadong Ma. 2023. Thinking image color aesthetics assessment: Models, datasets and benchmarks. In *Proceedings of the IEEE/CVF International Conference on Computer Vision*. 21838–21847.
- [18] Shuai He, Yongchang Zhang, Rui Xie, Dongxiang Jiang, and Anlong Ming. 2022. Rethinking Image Aesthetics Assessment: Models, Datasets and Benchmarks.. In *IJCAI*. 942–948.
- [19] Vlad Hosu, Bastian Goldlücke, and Dietmar Saupe. 2019. Effective aesthetics prediction with multi-level spatially pooled features. In *proceedings of the IEEE/CVF conference on computer vision and pattern recognition*. 9375–9383.
- [20] Vlad Hosu, Hanhe Lin, Tamas Sziranyi, and Dietmar Saupe. 2020. KonIQ-10k: An ecologically valid database for deep learning of blind image quality assessment. *IEEE TIP* 29 (2020), 4041–4056.
- [21] Byungho Jo, Donghyeon Cho, In Kyu Park, and Sungeun Hong. 2023. IFQA: interpretable face quality assessment. In *Proceedings of the IEEE/CVF winter conference on applications of computer vision*. 3444–3453.
- [22] Junjie Ke, Qifei Wang, Yilin Wang, Peyman Milanfar, and Feng Yang. 2021. Musiq: Multi-scale image quality transformer. In *Proceedings of the IEEE/CVF international conference on computer vision*. 5148–5157.
- [23] Junjie Ke, Keren Ye, Jiahui Yu, Yonghui Wu, Peyman Milanfar, and Feng Yang. 2023. Vila: Learning image aesthetics from user comments with vision-language pretraining. In *Proceedings of the IEEE/CVF Conference on Computer Vision and Pattern Recognition*. 10041–10051.
- [24] Diederik P Kingma. 2014. Adam: A method for stochastic optimization. *arXiv preprint arXiv:1412.6980* (2014).
- [25] Shu Kong, Xiaohui Shen, Zhe Lin, Radomir Mech, and Charless Fowlkes. 2016. Photo aesthetics ranking network with attributes and content adaptation. In *ECCV*. Springer, 662–679.
- [26] Eric C Larson and Damon M Chandler. 2010. Most apparent distortion: full-reference image quality assessment and the role of strategy. *Journal of electronic imaging* 19, 1 (2010), 011006–011006.
- [27] Chunyi Li, Zicheng Zhang, Haoning Wu, Wei Sun, Xiongkuo Min, Xiaohong Liu, Guangtao Zhai, and Weisi Lin. 2023. Agiqa-3k: An open database for ai-generated image quality assessment. *IEEE Transactions on Circuits and Systems for Video Technology* (2023).
- [28] Dingquan Li, Tingting Jiang, Weisi Lin, and Ming Jiang. 2018. Which has better visual quality: The clear blue sky or a blurry animal? *IEEE Transactions on Multimedia* 21, 5 (2018), 1221–1234.
- [29] Leida Li, Yipo Huang, Jinjian Wu, Yuzhe Yang, Yaqian Li, Yandong Guo, and Guangming Shi. 2023. Theme-aware visual attribute reasoning for image aesthetics assessment. *IEEE Transactions on Circuits and Systems for Video Technology* 33, 9 (2023), 4798–4811.
- [30] Youwei Liang, Junfeng He, Gang Li, Peizhao Li, Arseniy Klimovskiy, Nicholas Carolan, Jiao Sun, Jordi Pont-Tuset, Sarah Young, Feng Yang, et al. 2024. Rich human feedback for text-to-image generation. In *Proceedings of the IEEE/CVF Conference on Computer Vision and Pattern Recognition*. 19401–19411.
- [31] Hanhe Lin, Vlad Hosu, and Dietmar Saupe. 2019. KADID-10k: A large-scale artificially distorted IQA database. In *2019 Eleventh International Conference on Quality of Multimedia Experience (QoMEX)*. IEEE, 1–3.
- [32] Limin Liu, Shuai He, Anlong Ming, Rui Xie, and Huadong Ma. 2024. ELTA: an enhancer against long-tail for aesthetics-oriented models. In *Forty-first International Conference on Machine Learning*.
- [33] Lixiong Liu, Tianshu Wang, and Hua Huang. 2019. Pre-attention and spatial dependency driven no-reference image quality assessment. *IEEE Transactions on Multimedia* 21, 9 (2019), 2305–2318.
- [34] Qidong Liu, Xian Wu, Xiangyu Zhao, Yuanshao Zhu, Derong Xu, Feng Tian, and Yefeng Zheng. 2024. When MOE Meets LLMs: Parameter Efficient Fine-tuning for Multi-task Medical Applications. In *Proceedings of the 47th International ACM SIGIR Conference on Research and Development in Information Retrieval*. 1104–1114.
- [35] Yutao Liu, Ke Gu, Jingchao Cao, Shiqi Wang, Guangtao Zhai, Junyu Dong, and Sam Kwong. 2023. UIQI: A comprehensive quality evaluation index for underwater images. *IEEE Transactions on Multimedia* (2023).
- [36] Xiongkuo Min, Ke Gu, Guangtao Zhai, Jing Liu, Xiaokang Yang, and Chang Wen Chen. 2017. Blind quality assessment based on pseudo-reference image. *IEEE Transactions on Multimedia* 20, 8 (2017), 2049–2062.
- [37] Xiongkuo Min, Guangtao Zhai, Ke Gu, Xiaokang Yang, and Xinping Guan. 2018. Objective quality evaluation of dehazed images. *IEEE Transactions on Intelligent Transportation Systems* 20, 8 (2018), 2879–2892.
- [38] Anish Mittal, Anush Krishna Moorthy, and Alan Conrad Bovik. 2012. No-reference image quality assessment in the spatial domain. *IEEE Transactions on image processing* 21, 12 (2012), 4695–4708.
- [39] Naila Murray, Luca Marchesotti, and Florent Perronnin. 2012. AVA: A large-scale database for aesthetic visual analysis. In *CVPR*. IEEE, 2408–2415.
- [40] Fu-Zhao Ou, Xingyu Chen, Ruixin Zhang, Yuge Huang, Shaoxin Li, Jilin Li, Yong Li, Liujuan Cao, and Yuan-Gen Wang. 2021. SDD-FIQA: Unsupervised face image quality assessment with similarity distribution distance. In *Proceedings of the IEEE/CVF conference on computer vision and pattern recognition*. 7670–7679.
- [41] Wensheng Pan, Timin Gao, Yan Zhang, Runze Hu, Xiawu Zheng, Enwei Zhang, Yuting Gao, Yutao Liu, Yunhang Shen, Ke Li, et al. 2024. Multi-Modal Prompt Learning on Blind Image Quality Assessment. *arXiv preprint arXiv:2404.14949* (2024).
- [42] Nikolay Ponomarenko, Oleg Ieremeiev, Vladimir Lukin, Karen Egiazarian, Lina Jin, Jaakko Astola, Benoit Vozel, Kacem Chehdi, Marco Carli, Federica Battisti, et al. 2013. Color image database TID2013: Peculiarities and preliminary results. In *European workshop on visual information processing (EUVIP)*. IEEE, 106–111.
- [43] Guanyi Qin, Runze Hu, Yutao Liu, Xiawu Zheng, Haotian Liu, Xiu Li, and Yan Zhang. 2023. Data-efficient image quality assessment with attention-panel decoder. In *Proceedings of the AAAI Conference on Artificial Intelligence*, Vol. 37. 2091–2100.
- [44] Alec Radford, Jong Wook Kim, Chris Hallacy, Aditya Ramesh, Gabriel Goh, Sandhini Agarwal, Girish Sastry, Amanda Askell, Pamela Mishkin, Jack Clark, et al. 2021. Learning transferable visual models from natural language supervision. In *International conference on machine learning*. PMLR, 8748–8763.
- [45] Carlos Riquelme, Joan Puigcerver, Basil Mustafa, Maxim Neumann, Rodolphe Jenatton, André Susano Pinto, Daniel Keysers, and Neil Houlsby. 2021. Scaling vision with sparse mixture of experts. *Advances in Neural Information Processing*

- Systems* 34 (2021), 8583–8595.
- [46] Robin Rombach, Andreas Blattmann, Dominik Lorenz, Patrick Esser, and Björn Ommer. 2022. High-resolution image synthesis with latent diffusion models. In *Proceedings of the IEEE/CVF conference on computer vision and pattern recognition*. 10684–10695.
- [47] Noam Shazeer, Azalia Mirhoseini, Krzysztof Maziarz, Andy Davis, Quoc Le, Geoffrey Hinton, and Jeff Dean. 2017. Outrageously large neural networks: The sparsely-gated mixture-of-experts layer. *arXiv preprint arXiv:1701.06538* (2017).
- [48] Hamid R Sheikh, Muhammad F Sabir, and Alan C Bovik. 2006. A statistical evaluation of recent full reference image quality assessment algorithms. *IEEE TIP* 15, 11 (2006), 3440–3451.
- [49] Kekai Sheng, Weiming Dong, Chongyang Ma, Xing Mei, Feiyue Huang, and Bao-Gang Hu. 2018. Attention-based multi-patch aggregation for image aesthetic assessment. In *Proceedings of the 26th ACM international conference on Multimedia*. 879–886.
- [50] Shaolin Su, Hanhe Lin, Vlad Hosu, Oliver Wiedemann, Jinqiu Sun, Yu Zhu, Hantao Liu, Yanning Zhang, and Dietmar Saupe. 2023. Going the extra mile in face image quality assessment: A novel database and model. *IEEE Transactions on Multimedia* (2023).
- [51] Shaolin Su, Hanhe Lin, Vlad Hosu, Oliver Wiedemann, Jinqiu Sun, Yu Zhu, Hantao Liu, Yanning Zhang, and Dietmar Saupe. 2023. Going the extra mile in face image quality assessment: A novel database and model. *IEEE TMM* (2023).
- [52] Shaolin Su, Qingsen Yan, Yu Zhu, Cheng Zhang, Xin Ge, Jinqiu Sun, and Yanning Zhang. 2020. Blindly assess image quality in the wild guided by a self-adaptive hyper network. In *Proceedings of the IEEE/CVF conference on computer vision and pattern recognition*. 3667–3676.
- [53] Wei Sun, Xiongkuo Min, Danyang Tu, Siwei Ma, and Guangtao Zhai. 2023. Blind quality assessment for in-the-wild images via hierarchical feature fusion and iterative mixed database training. *IEEE Journal of Selected Topics in Signal Processing* 17, 6 (2023), 1178–1192.
- [54] Hossein Talebi and Peyman Milanfar. 2018. NIMA: Neural image assessment. *IEEE transactions on image processing* 27, 8 (2018), 3998–4011.
- [55] Longxiang Tang, Zhuotao Tian, Kai Li, Chunming He, Hantao Zhou, Hengshuang Zhao, Xiu Li, and Jiaya Jia. 2024. Mind the interference: Retaining pre-trained knowledge in parameter efficient continual learning of vision-language models. In *European Conference on Computer Vision*. Springer, 346–365.
- [56] Zhengzhong Tu, Hossein Talebi, Han Zhang, Feng Yang, Peyman Milanfar, Alan Bovik, and Yinxiao Li. 2022. Maxvit: Multi-axis vision transformer. In *European conference on computer vision*. Springer, 459–479.
- [57] Jianyi Wang, Kelvin CK Chan, and Chen Change Loy. 2023. Exploring clip for assessing the look and feel of images. In *Proceedings of the AAAI Conference on Artificial Intelligence*, Vol. 37. 2555–2563.
- [58] Wenhui Wang, Hangbo Bao, Li Dong, Johan Bjorck, Zhiliang Peng, Qiang Liu, Kriti Aggarwal, Owais Khan Mohammed, Saksham Singhal, Subhojit Som, et al. 2022. Image as a foreign language: Beit pretraining for all vision and vision-language tasks. *arXiv preprint arXiv:2208.10442* (2022).
- [59] Haoning Wu, Zicheng Zhang, Weixia Zhang, Chaofeng Chen, Liang Liao, Chunyi Li, Yixuan Gao, Annan Wang, Erli Zhang, Wenxiu Sun, et al. 2023. Q-align: Teaching llms for visual scoring via discrete text-defined levels. *arXiv preprint arXiv:2312.17090* (2023).
- [60] Yicheng Xiao, Zhuoyan Luo, Yung Liu, Yue Ma, Hengwei Bian, Yatai Ji, Yujiu Yang, and Xiu Li. 2024. Bridging the gap: A unified video comprehension framework for moment retrieval and highlight detection. In *Proceedings of the IEEE/CVF Conference on Computer Vision and Pattern Recognition*. 18709–18719.
- [61] Yicheng Xiao, Yue Ma, Shuyan Li, Hantao Zhou, Ran Liao, and Xiu Li. 2023. Semanticac: semantics-assisted framework for audio classification. In *ICASSP 2023-2023 IEEE International Conference on Acoustics, Speech and Signal Processing (ICASSP)*. IEEE, 1–5.
- [62] Yicheng Xiao, Lin Song, Rui Yang, Cheng Cheng, Zunnan Xu, Zhaoyang Zhang, Yixiao Ge, Xiu Li, and Ying Shan. 2025. Haploomni: Unified single transformer for multimodal video understanding and generation. *arXiv preprint arXiv:2506.02975* (2025).
- [63] Kangmin Xu, Liang Liao, Jing Xiao, Chaofeng Chen, Haoning Wu, Qiong Yan, and Weisi Lin. 2024. Boosting Image Quality Assessment through Efficient Transformer Adaptation with Local Feature Enhancement. In *Proceedings of the IEEE/CVF Conference on Computer Vision and Pattern Recognition*. 2662–2672.
- [64] Lingxiao Yang, Ru-Yuan Zhang, Yan Chen Wang, and Xiaohua Xie. 2024. MMA: Multi-Modal Adapter for Vision-Language Models. In *Proceedings of the IEEE/CVF Conference on Computer Vision and Pattern Recognition*. 23826–23837.
- [65] Miao Yang and Arcot Sowmya. 2015. An underwater color image quality evaluation metric. *IEEE Transactions on Image Processing* 24, 12 (2015), 6062–6071.
- [66] Ning Yang, Qihang Zhong, Kun Li, Runmin Cong, Yao Zhao, and Sam Kwong. 2021. A reference-free underwater image quality assessment metric in frequency domain. *Signal Processing: Image Communication* 94 (2021), 116218.
- [67] Ning Yang, Qihang Zhong, Kun Li, Runmin Cong, Yao Zhao, and Sam Kwong. 2021. A reference-free underwater image quality assessment metric in frequency domain. *Signal Processing: Image Communication* 94 (2021), 116218.
- [68] Rui Yang, Lin Song, Yanwei Li, Sijie Zhao, Yixiao Ge, Xiu Li, and Ying Shan. 2024. Gpt4tools: Teaching large language model to use tools via self-instruction. *Advances in Neural Information Processing Systems* 36 (2024).
- [69] Rui Yang, Lin Song, Yicheng Xiao, Runhui Huang, Yixiao Ge, Ying Shan, and Hengshuang Zhao. 2025. Haplovl: A single-transformer baseline for multi-modal understanding. *arXiv preprint arXiv:2503.14694* (2025).
- [70] Ran Yi, Haoyuan Tian, Zhihao Gu, Yu-Kun Lai, and Paul L Rosin. 2023. Towards artistic image aesthetics assessment: a large-scale dataset and a new method. In *Proceedings of the IEEE/CVF Conference on Computer Vision and Pattern Recognition*. 22388–22397.
- [71] Zhenqiang Ying, Haoran Niu, Praful Gupta, Dhruv Mahajan, Deepti Ghadiyaram, and Alan Bovik. 2020. From patches to pictures (PaQ-2-PiQ): Mapping the perceptual space of picture quality. In *CVPR*. 3575–3585.
- [72] Zhiyuan You, Zheyuan Li, Jinjin Gu, Zhenfei Yin, Tianfan Xue, and Chao Dong. 2023. Depicting beyond scores: Advancing image quality assessment through multi-modal language models. *arXiv preprint arXiv:2312.08962* (2023).
- [73] Jiquan Yuan, Xinyan Cao, Linjing Cao, Jinlong Lin, and Xixin Cao. 2023. Pscr: Patches sampling-based contrastive regression for aigc image quality assessment. *arXiv preprint arXiv:2312.05897* (2023).
- [74] Guanghui Yue, Di Cheng, Tianwei Zhou, Jingwen Hou, Weide Liu, Long Xu, Tianfu Wang, and Jun Cheng. 2023. Perceptual quality assessment of enhanced colonoscopy images: A benchmark dataset and an objective method. *IEEE Transactions on Circuits and Systems for Video Technology* 33, 10 (2023), 5549–5561.
- [75] Weixia Zhang, Kede Ma, Jia Yan, Dexiang Deng, and Zhou Wang. 2018. Blind image quality assessment using a deep bilinear convolutional neural network. *IEEE TCSVT* 30, 1 (2018), 36–47.
- [76] Weixia Zhang, Kede Ma, Guangtao Zhai, and Xiaokang Yang. 2021. Uncertainty-aware blind image quality assessment in the laboratory and wild. *IEEE Transactions on Image Processing* 30 (2021), 3474–3486.
- [77] Weixia Zhang, Guangtao Zhai, Ying Wei, Xiaokang Yang, and Kede Ma. 2023. Blind image quality assessment via vision-language correspondence: A multitask learning perspective. In *Proceedings of the IEEE/CVF conference on computer vision and pattern recognition*. 14071–14081.
- [78] Zicheng Zhang, Yingjie Zhou, Chunyi Li, Baixuan Zhao, Xiaohong Liu, and Guangtao Zhai. 2024. Quality assessment in the era of large models: A survey. *ACM Transactions on Multimedia Computing, Communications and Applications* (2024).
- [79] Shiyu Zhao, Lin Zhang, Shuaiyi Huang, Ying Shen, and Shengjie Zhao. 2020. Dehazing evaluation: Real-world benchmark datasets, criteria, and baselines. *IEEE Transactions on Image Processing* 29 (2020), 6947–6962.
- [80] Shiyu Zhao, Lin Zhang, Ying Shen, and Yicong Zhou. 2021. RefineDNet: A weakly supervised refinement framework for single image dehazing. *IEEE Transactions on Image Processing* 30 (2021), 3391–3404.
- [81] Hantao Zhou, Runze Hu, and Xiu Li. 2024. Video object segmentation with dynamic query modulation. In *2024 IEEE International Conference on Multimedia and Expo (ICME)*. IEEE, 1–6.
- [82] Hantao Zhou, Longxiang Tang, Rui Yang, Guanyi Qin, Yan Zhang, Runze Hu, and Xiu Li. 2024. UniQA: Unified Vision-Language Pre-training for Image Quality and Aesthetic Assessment. *arXiv preprint arXiv:2406.01069* (2024).
- [83] Hantao Zhou, Rui Yang, Runze Hu, Chang Shu, Xiaochu Tang, and Xiu Li. 2023. Etdnet: Efficient transformer-based detection network for surface defect detection. *IEEE transactions on instrumentation and measurement* 72 (2023), 1–14.
- [84] Hantao Zhou, Rui Yang, Yachao Zhang, Haoran Duan, Yawen Huang, Runze Hu, Xiu Li, and Yefeng Zheng. 2024. Unihead: unifying multi-perception for detection heads. *IEEE Transactions on Neural Networks and Learning Systems* (2024).
- [85] Hancheng Zhu, Leida Li, Jinjian Wu, Sicheng Zhao, Guiguang Ding, and Guangming Shi. 2020. Personalized image aesthetics assessment via meta-learning with bilevel gradient optimization. *IEEE Transactions on Cybernetics* 52, 3 (2020), 1798–1811.

A MORE IMPLEMENTATION DETAILS

Table 10: Training settings for different datasets.

Dataset	Task	Epoch	Batch size
LIVE [48]	SDN-IQA	50	8
CSIQ [26]	SDN-IQA	50	8
TID2013 [42]	SDN-IQA	20	8
KADID [31]	SDN-IQA	20	8
CLIVE [12]	ADN-IQA	50	8
KonIQ [20]	ADN-IQA	20	8
SPAQ [10]	ADN-IQA	20	8
GFIQA20k [50]	F-IQA	10	8
AGIQA3k [27]	AG-IQA	20	8
UWIQA [66]	U-IQA	50	8
AVA [39]	IAA	20	128
AADB [25]	IAA	20	8
exBeDDE [79]	D-IQA	20	8
ECIQAD [74]	EC-IQA	20	8

Table 11: Detail information about the 14 used datasets.

Dataset	Task	Image Number	MOS Type	Range
LIVE [48]	SDN-IQA	779	DMOS	[1, 100]
CSIQ [26]		866	DMOS	[0, 1]
TID2013 [42]		3,000	MOS	[0, 9]
KADID-10k [31]		10,125	MOS	[1, 5]
SPAQ [10]	ADN-IQA	11,125	MOS	[0, 100]
LIVEC [12]		1,162	MOS	[1, 100]
KonIQ-10K [20]		10,073	MOS	[0, 100]
GFIQA20k [51]	F-IQA	19,988	MOS	[0, 1]
AGIQA3k [27]	AG-IQA	2,982	MOS	[0, 1]
UWIQA [66]	U-IQA	890	MOS	[0, 1]
AVA [39]	IAA	250,000	MOS	[0, 10]
AADB [25]	IAA	10,000	MOS	[0, 1]
exBeDDE [79]	D-IQA	1670	MOS	[0, 1]
ECIQAD [74]	EC-IQA	2400	MOS	[1, 9]

A.1 Evaluation Criteria

We use Spearman’s Rank-Order Correlation Coefficient (SRCC) and Pearson’s Linear Correlation Coefficient (PLCC) as criteria to measure the performance of IQA models. Both coefficients range from 0 to 1, with higher values indicating better performance. We randomly crop a 224x224 image patch from the original image and perform score prediction, following [43, 77]. This process is repeated 10 times, and the average of the 10 predicted scores is used as the final quality score of the image.

A.2 Training Details

We follow the typical training strategy to fine-tune each dataset, including random cropping and random horizontal flipping. We

Table 12: Cross-dataset validation when using the same training data as LIQE [77] and UNIQUE [76]. The subscripts “s” and “r” stand for models trained on KADID and KonIQ, respectively. Gamma[†] uses the same 6 datasets as LIQE and UNIQUE for training and validation. Gamma^{††} uses 12 datasets (include TID2012 and SPAQ) for training and performs zero-shot cross dataset validation on other datasets. Gamma^{††} significantly enhances the zero-shot performance on other datasets, showing the effectiveness of mix-training via MoAE and SDP.

Dataset	TID2013	SPAQ	AIGC2023	Average
NIQE	0.314	0.578	-	0.446
DBCNN _s	0.686	0.412	0.730	0.609
PaQ2PiQ	0.423	0.823	0.643	0.630
MUSIQ _r	0.584	0.853	0.736	0.724
UNIQUE	0.768	0.838	0.761	0.789
LIQE	0.811	0.881	0.744	0.812
Gamma [†]	0.805	0.894	0.770	0.823
Gamma ^{††}	-	-	0.818	-

Table 13: Generalization capability validation on the BAID [70] and ICAA17K [17] datasets. We use the pre-trained weight of Gamma for model initialization.

(a) Results on the BAID dataset.

Method	SRCC	PLCC
NIMA [54]	0.393	0.382
MP _{ada} [49]	0.437	0.425
MLSP [19]	0.441	0.430
BIAA [85]	0.389	0.376
TANet [18]	0.453	0.437
BAID [70]	0.473	0.467
Ours	0.496	0.556

(b) Results on the ICAA17K dataset.

Method	SRCC	PLCC
NIMA [54]	0.809	0.815
MP _{ada} [49]	0.810	0.819
MLSP [19]	0.826	0.837
BIAA [85]	0.820	0.829
MUSIQ [22]	0.835	0.841
TANet [18]	0.829	0.836
MaxViT [56]	0.855	0.874
ICAA [17]	0.873	0.890
Ours	0.877	0.893

conduct all experiments on 3090 GPU. Mixed training of the 12 datasets takes 10 hours on a 3090 GPU. For the task-specific training, Table 10 shows the detailed training setting for the different datasets. We use the learning rate of 2e-5 for all datasets.

A.3 Datasets

In this paper, we use a total of 14 datasets, 12 of which are used for unified training and 2 are used to evaluate the generalization

Table 14: Text prompts used in Scene-based Differential Prompt.

Dataset	Prompt
LIVE, CSIQ, TID2013, KADID LIVEC, KonIQ, SPAQ	{natural bad-quality image, natural poor-quality image, natural fair-quality image, natural good-quality image, natural perfect-quality image}
AGIQA3k	{AI-generated bad-quality image, AI-generated poor-quality image, AI-generated fair-quality image, AI-generated good-quality image, AI-generated perfect-quality image}
GFIQA20k	{face bad-quality image, face poor-quality image, face fair-quality image, face good-quality image, face perfect-quality image}
UWIQA	{underwater bad-quality image, underwater poor-quality image, underwater fair-quality image, underwater good-quality image, underwater perfect-quality image}
AVA, AADB	{natural bad-aesthetics image, natural poor-aesthetics image, natural fair-aesthetics image, natural good-aesthetics image, natural perfect-aesthetics image}

Table 15: Model complexity comparison with LIQE and Q-Align.

Method	Trainable Parms	FLOPs	Inference time	KonIQ SRCC	KADID SRCC
Q-Align [59]	8.2B (8200M)	-	0.1s	0.938	0.934
LIQE [77]	151M	17.40G	0.02s	0.919	0.930
Gamma	122.8M	28.45G	0.025s	0.939	0.962

Table 16: Sensitivity analysis of prompt. Quality prompt is {bad-quality, poor-quality, fair-quality, good-quality, perfect-quality}; General prompt replaces the scene prompt (see Table 14) to “general”, e.g., {underwear bad-quality image} to {general bad-quality image}.

Dataset	LIVEC		KonIQ		LIVE		CSIQ		AGIQA3k		UWIQA		AVA	
	SRCC	PLCC	SRCC	PLCC	SRCC	PLCC	SRCC	PLCC	SRCC	PLCC	SRCC	PLCC	SRCC	PLCC
General prompt	0.882	0.888	0.921	0.920	0.943	0.930	0.948	0.957	0.775	0.843	0.832	0.842	0.648	0.624
Quality prompt	0.885	0.889	0.931	0.940	0.950	0.946	0.946	0.951	0.822	0.872	0.861	0.876	0.451	0.455
SDP	0.891	0.914	0.939	0.950	0.953	0.953	0.960	0.968	0.887	0.923	0.873	0.884	0.750	0.749

ability of our model. We present the details of the used datasets in Table 11.

A.4 Details of the Scene-based Differential Prompt

In the Scene-based Differential Prompt, we use different prompts for datasets from different scene. Specifically, we divide datasets into five categories, *i.e.*, natural IQA, AI-generated IQA, underwater IQA, face IQA, natural IAA. We present the details in Table 14.

B CROSS DATASET VALIDATION

We conduct cross dataset validation to evaluate the generalization ability of our method. We compare with LIQE and UNIQUE using the same training data and data splitting ratios. As shown in Table 12, our method achieves highly competitive results on TID2013 and SPAQ, demonstrating the strong generalization capability of

our method. Note that using mix-training of more dataset can significantly enhance the zero-shot performance on other datasets, *i.e.*, 0.770 SRCC to 0.818 SRCC on AIGC2023 dataset, demonstrating the effectiveness of mix-training via MoAE and SDP methods.

C MORE GENERALIZATION CAPABILITY VALIDATION

Gamma can be used as a pre-trained model and easily applied to new tasks after fine-tuning. We select the artistic IAA dataset BAID [70] and color IAA dataset ICAA17K [17] for further performance evaluation. BAID is a large-scale artistic image aesthetics assessment (AIAA) dataset, which consists of 60,337 artistic images covering various art forms. ICAA17K is a color-oriented IAA dataset, containing 17K images. We fine-tune Gamma for 10 epochs on them. As shown in the Table 13, Gamma achieves SOTA performance on two datasets, although it is not specifically designed for them.

These results further verify the powerful generalization ability of Gamma.

D MODEL EFFICIENCY ANALYSIS

We calculate the number of parameters, computation, and inference time of our model. For inference time, we use a 224×224 image for testing. All indicators are obtained on a 3090 GPU. We compare it with two classic mixed training methods, LIQE [77] and Q-Align [59]. As shown in Table 15, our model achieves the best accuracy and efficiency. Compared with LIQE, our model has significantly better performance. Compared with Q-Align, we not only have better performance, but also have significantly lower model parameters and inference latency.

E SENSITIVITY ANALYSIS OF PROMPT

We analyze the sensitivity of prompts when the model is trained with scene-based differential prompts (SDP). Table 16 shows that using prompts different from SDP slightly reduces performance on most datasets, showing the robustness of our method. The quality prompt performs better than the general prompt on the IQA task, but performs worse on the IAA task, indicating the importance of appropriate prompts. In conclusion, our method is robust and insensitive to prompts, nevertheless we suggest using correct prompts to obtain better performance.